

Optimum Criteria on the Performance of an Irreversible Braysson Heat Engine Based on the New Thermoeconomic Approach

Sudhir Kumar Tyagi^{1,2}, Yinghui Zhou¹ and Jincan Chen^{1*}

1. Department of Physics, Xiamen University, Xiamen 361005, People's Republic of China
 2. Centre for Energy Studies, Indian Institute of Technology, Delhi New Delhi 110016, India
- * The corresponding author Tel: +86-592-218-9426, Fax: +86-592-218-9426, E-mail address: jcchen@xmu.edu.cn (Jincan Chen) and sudhirtyagi@yahoo.com (S. K. Tyagi)

Received: 28 January 2004 / Accepted: 8 March 2004 / Published: 17 March 2004

Abstract

An irreversible cycle model of a Braysson heat engine operating between two heat reservoirs is used to investigate the thermoeconomic performance of the cycle affected by the finite-rate heat transfer between the working fluid and the heat reservoirs, heat leak loss from the heat source to the ambient and the irreversibility within the cycle. The thermoeconomic objective function, defined as the total cost per unit power output, is minimized with respect to the cycle temperatures along with the isobaric temperature ratio for a given set of operating parameters. The objective function is found to be an increasing function of the internal irreversibility parameter, economic parameters and the isobaric temperature ratio. On the other hand, there exist the optimal values of the state point temperatures, power output and thermal efficiency at which the objective function attains its minimum for a typical set of operating parameters. Moreover, the objective function and the corresponding power output are also plotted against the state point temperature and thermal efficiency for a different set of operating parameters. The optimally operating regions of these important parameters in the cycle are also determined. The results obtained here may provide some useful criteria for the optimal design and performance improvements, from the point of view of economics as well as from the point of view of thermodynamics of an irreversible Braysson heat engine cycle and other similar cycles as well.

Keywords: Braysson heat engine, thermoeconomic objective function, power output, multi-irreversibilities, thermal efficiency, optimal operating region, optimum criterion

Nomenclature

A = Area (m²)

a's = Cost parameters

c_p = Specific heat (kJ/kg-K)

C's = Cost parameters

C_T = Total cost (defined in Eq.10)

F = Objective function (defined in Eq.12)

NCU = National Currency Unit

P = Power output (kW)

P* = Dimensionless power output

Q = Heat transfer rates (kW)

R = Internal irreversibility parameter

S = Entropy (kJ/K)

T = Temperature (K)

U = Overall heat transfer coefficient ($\text{kW/m}^2\text{-K}$) = Sink/cold -side

x = Isobaric temperature ratio

1, 2, 3, 4 = State points

Greeks

η = Efficiency

Subscripts

a = Ambient

c = Compressor

H = Heat source/hot-side

m=Related to the minimum objective function/maintenance

max = Maximum

min = Minimum

opt = Optimum

p = Related to power production cost

q = Related to input energy rate cost

Introduction

The Braysson cycle is a hybrid power cycle based on a conventional Brayton cycle for the high temperature heat addition while adopting the Ericsson cycle for the low temperature heat rejection as proposed and investigated by Frost et al. [1] using the first law of thermodynamics. Very recently, some workers [2-3] have investigated the performance of an endoreversible Braysson cycle based on the analysis of the Brayton [4-23] and Ericsson [24-28] cycles using the concept of finite time thermodynamics [29-33] for a typical set of operating conditions and obtained some significant results.

In real thermodynamic cycles, there often exist other irreversibilities besides finite-rate heat transfer between the working fluid and the heat reservoirs. For example, the heat leak loss from the heat source to the ambient and the internal dissipation of the working fluid are also another main source of irreversibility. In the present paper, we will study the influence of multi-irreversibilities on the thermoeconomic performance of a Braysson heat engine cycle.

An Irreversible Braysson Cycle

An irreversible Braysson cycle working between a source and a sink of infinite heat capacities is shown on the T-S diagram of Fig.1. The external irreversibilities are due to the finite temperature difference between the heat engine and the external reservoirs and the direct heat leak loss from the source to the ambient while the internal irreversibilities are due to the nonisentropic processes in the expander and compressor devices as well as due to other entropy generations within the cycle. The working fluid enters the compressor at state point 4 and is compressed up to state point 1S/1 in an ideal/real compressor, and then it comes into contact with the heat source and is heated up to state point 2 at constant pressure. After that the working fluid enters the turbine at state point 2 and expands up to state point 3S/3 in an ideal/real expander/turbine, it rejects the heat to the heat sink at constant temperature and enters the compressor at state point 4, thereby, completing the cycle. Thus, we will study the 4-1-2-3-4 closed cycle of an irreversible Braysson heat engine coupled with the heat reservoirs of infinite heat capacities at temperature T_H and T_L respectively.

Assuming the working fluid as an ideal/perfect gas, the heat transfer rates to and from the heat engine following Newton's Law of heat transfer [1-3, 30-36] will be:

$$Q_H = \frac{U_H A_H (T_2 - T_1)}{\ln \left(\frac{T_H - T_1}{T_H - T_2} \right)} = \dot{m} c_p (T_2 - T_1) \quad (1)$$

$$Q_L = U_L A_L (T_3 - T_L) \quad (2)$$

where $(UA)_J$ ($J = H, L$) are the overall heat transfer coefficient-area products on their respective side heat exchanger, T_i ($i = 1, 2, 3$) are the temperatures of the working fluid at state points 1, 2 and 3, and \dot{m} and c_p are, respectively, the mass flow rate and specific heat of the working fluid.

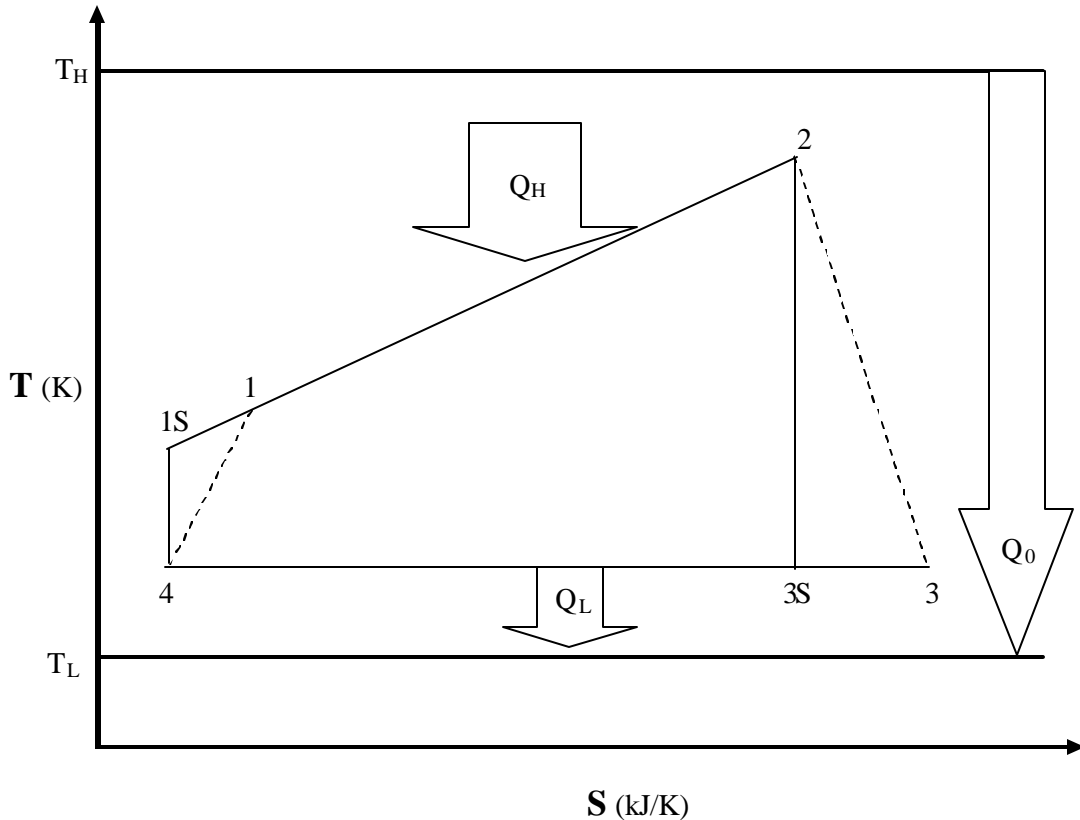


Fig.1: The T-S diagram of an irreversible Braysson heat engine cycle.

According to Fig.1, It is reasonable to consider some heat leak loss directly from the source to the ambient, which may be expressed as [27]:

$$Q_0 = k_0(T_H - T_a) \tag{3}$$

where k_0 is the heat leak coefficient and T_a is the ambient temperature and is usually the same as the sink temperature (T_L). In addition, it is also very important to further consider the influence of irreversible adiabatic processes and other entropy generations within the cycle. Assuming the working fluid as an ideal gas, the entropy production for the process 1-2 at constant pressure is:

$$TdS = dH - VdP \Rightarrow \Delta S_{1-2} = \dot{m}c_p \ln(x) \tag{4(a)}$$

where $x = T_2/T_1$ is the isobaric temperature ratio. Using the second law of thermodynamics for this cycle model, we have:

$$\dot{m}c_p \ln(x) - U_L A_L (T_3 - T_L)/T_3 < 0 \Rightarrow \dot{m}c_p R T_3 \ln(x) = U_L A_L (T_3 - T_L) \tag{4(b)}$$

where R is the internal irreversibility parameter which is greater than unity for a real cycle and defined as:

$$R = \frac{U_L A_L (T_3 - T_L)}{\dot{m}c_p \ln(x) T_3} > 1 \tag{5}$$

When the adiabatic processes are reversible and other entropy generations within the cycle are negligible, $R = 1$ and the cycle becomes an endoreversible cycle, in which the irreversibility is only due to finite temperature differences between the heat engine and the external reservoirs and the heat leak loss directly from the heat source to the ambient.

The Expressions of Several Parameters

Using Eqs.(1)-(3) and (5), we can derive the expressions of the power output and thermal efficiency, which are, respectively, given by:

$$P = Q_H - Q_L = \frac{U_H A [(x-1)T_1 - RT_3 \ln x]}{aT_3 / (T_3 - T_L) + b} \tag{6}$$

$$h = \frac{Q_H - Q_L}{Q_H + Q_0} = \frac{(x-1)T_1 - RT_3 \ln x}{(x-1)T_1 + \frac{k_0(T_H - T_L)}{U_H A} [aT_3 / (T_3 - T_L) + b]} \tag{7}$$

where $a = (U_H / U_L)R \ln x$, $b = \ln[(T_H - T_1)/(T_H - T_1x)]$ and $A = A_H + A_L$ is the total heat transfer area of the cycle. Using Eqs.(1-2) and (5), we can also derive the expressions of the ratios of the hot- and cold-side heat exchanger areas to the total heat exchanger area as:

$$\frac{A_H}{A} = \frac{b}{aT_3 / (T_3 - T_L) + b} \tag{8}$$

$$\frac{A_L}{A} = \frac{aT_3 / (T_3 - T_L)}{aT_3 / (T_3 - T_L) + b} \tag{9}$$

The Thermo-economic Objective Function

Let C_T be the total cost of the heat engine system per unit time, which includes the costs of the hot- and cold-side heat exchangers (C_1), the costs of the compression/expansion device (C_2), the input energy cost (C_3) and the maintenance cost (C_4) of the system in such a way that these costs are proportional to the total conductance, the compression/expansion capacity, the amount of heat supplied by the heat source per cycle and the power output of the cycle respectively, viz. $C_1 \propto UA$, $C_2 \propto P$, $C_3 \propto (Q_H + Q_0)$ and $C_4 \propto P$. Thus, the total cost of the system can be expressed as:

$$C_T = C_1 + C_2 + C_3 + C_4 = a_H(UA)_H + a_L(UA)_L + a_p P + a_q(Q_H + Q_0) + a_m P \tag{10(a)}$$

where a_H and a_L are the proportional coefficients of the cost of the hot- and cold-side heat exchangers respectively, their units are NCU/(s-kW/K), a_p , a_q and a_m is the proportional coefficients of the costs of the compression/expansion device, input energy and maintenance, and their dimensions are NCU/(s-kW), here NCU is the National Currency Unit. Using Eqs.(1-2 and 5) and substituting $k_1 = a_L / a_H$, $k_2 = (a_p + a_m) / a_H$ and $k_3 = a_q / a_H$ into Eq.10(a), we have:

$$C_T = \frac{a_H Q_H}{(x-1)T_1} \left[b + RT_3 \ln x \left(\frac{k_1}{T_3 - T_L} - k_2 \right) + k_4 (x-1)T_1 + k_5 \left(\frac{aT_3}{T_3 - T_L} + b \right) \right] \tag{10(b)}$$

where $k_4 = k_2 + k_3$, $k_5 = k_3 u (T_H - T_L)$ and $u = k_0 / (U_H A)$. Again using Eqs.(1-2 and 5) and the first law of thermodynamics, yields:

$$P = Q_H - Q_L \Rightarrow P = Q_H \left(1 - \frac{Q_L}{Q_H} \right) \Rightarrow P = Q_H \left(1 - \frac{RT_3 \ln x}{(x-1)T_1} \right) \tag{11}$$

Using Eqs.10(b) and (11), the total cost of the system per unit work output may be expressed as $F' = C_T / P$. For the sake of simplification, the objective function F' can be changed as:

$$F = \frac{F'}{a_H} = \frac{RT_3 \ln x \left(\frac{k_6}{T_3 - T_L} - k_2 \right) + k_4 (x-1)T_1 + (1+k_5)b}{(x-1)T_1 - RT_3 \ln x} \tag{12}$$

where $k_6 = k_1 + k_5 U_H / U_L$ while F is referred to as the thermoeconomic objective function of an irreversible Braysson heat engine. The objective function defined in Eq.(12) is more general than those used by the earlier workers [35, 36]. For example, if $R = x = 1$ and $a_p = a_q = a_m = Q_0 = 0$ are chosen, then $1/F$ becomes the objective function used in Ref.[35]. When $R = x = 1$, $a_H = a_L$ and $a_p = a_m = Q_0 = 0$ are chosen, F becomes the objective function used in Ref. [36]. Again, if $x = 1$ and other parameters are same, this cycle model will reduce to an irreversible Carnot cycle.

Using the above equations, one can analyze the optimal performance of an irreversible Braysson heat engine cycle.

Optimal Performance Characteristics

It is seen from Eq.(12) that the objective function is a function of two variables (T_1, T_3) for given values of the isobaric temperature ratio x and other parameters. Using Eq.(12) and its extremal condition $\partial F / \partial T_3 = 0$, it can be proven that when the objective function is in the optimal states, the temperature T_3 should satisfy the following equation:

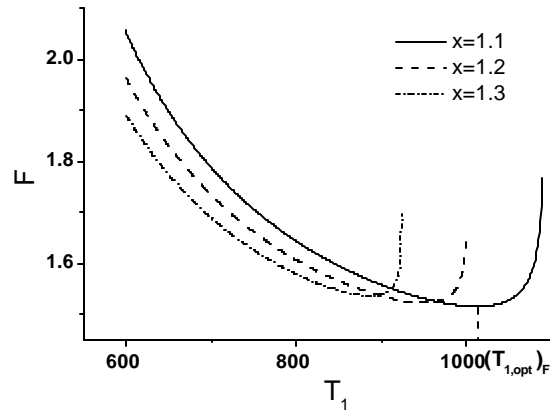
$$T_{3,opt} = \frac{a_1 T_L + \sqrt{a_1 k_6 T_L [(x-1)T_1 - RT_L \ln x] + Rk_6^2 T_L T_1 (x-1) \ln x}}{a_1 + k_6 R \ln x} \tag{13}$$

where $a_1 = (1 + k_5)b + k_3(x-1)T_1$. Using Eqs.(6, 12, 13), one can generate the graphs between the objective function and the state point temperature (T_1), between the corresponding power output and the state point temperature (T_1), between the objective function and corresponding thermal efficiency, between the objective function and corresponding power output as well as between the corresponding power output and corresponding thermal efficiency for a typical set of parameters viz. $T_H = 1200 K$, $T_L = T_a = 300 K$, $U_H / U_L = 1.0$, $k_1 = 1.1$, $k_2 = 0.6$, $k_3 = 0.5$ and $u = 0.01$, as shown in Figs. 2-5, where $P_m^* = P_m / (U_L A T_L)$, P_m is the power output corresponding to the minimum objective function, and $(h_m)_{max}$ and $(P_m^*)_{max}$ are, respectively, the maximum values of the thermal efficiency and power output at the minimum objective function.

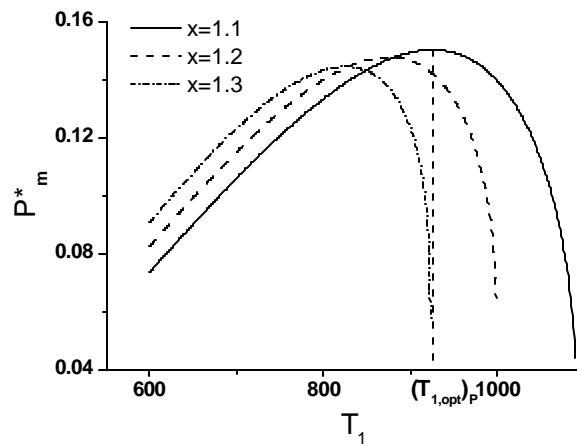
Minimum Value of Objective Function

The variations of the objective function and the corresponding dimensionless power output against the state point temperature (T_1) are shown in Figs.2-3. It is seen from these figures that the objective function first decreases and then increases while the corresponding power output first increases and then decreases as T_1 increases. It shows clearly that there are optimal values of T_1 at which the objective function and the

corresponding power output attain the minimum and maximum values for a given set of operating parameters, respectively. Also the optimal values of T_1 are different for different parameters at different operating condition.

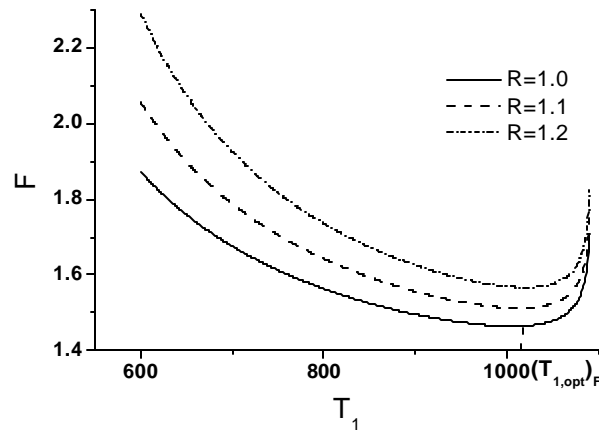


2(a)



2(b)

Fig.2. The variation of (a) the objective function and (b) the corresponding power output with respect to temperature T_1 for different values of the isobaric temperature ratio (x), where the parameters $T_H = 1200 K$, $T_L = 300 K$, $R = 1.1$, $U_H / U_L = 1.0$, $k_1 = 1.1$, $k_2 = 0.6$, $k_3 = 0.5$ and $u = 0.01$ are chosen.



3(a)

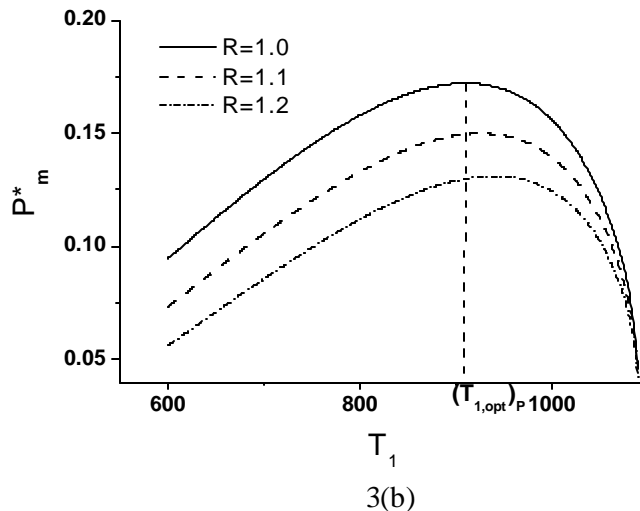


Fig.3 The variation of (a) the objective function and (b) the corresponding power output with respect to temperature T_1 for different values of R , where $x = 1.1$ and the values of the parameters are the same as those used in Fig. 2.

For example, the optimal value of T_1 at the minimum objective function is greater than that of T_1 at the corresponding maximum power output, i.e.

$$(T_{1,opt})_{P_m^*} \leq (T_{1,opt})_F \leq T_{1,max} \tag{14}$$

where $T_{1,max}$ are the maximum obtainable temperatures for a given set of operating parameters. Figures 2 and 3 show that $(T_{1,opt})_{P_m^*}$ and $(T_{1,opt})_F$ decreases with the increase of x and increases with the increase of R . Again, it is also seen from these figures that the objective function is a monotonically increasing function of both x and R while it is reverse in the case of the corresponding power output. This point is easily expounded from the theory of thermodynamics. Because the larger the internal irreversibility parameter R and the isobaric temperature ratio x are, the larger the total irreversibility in the cycle and consequently the smaller the corresponding power output and the larger will be the cost of the system and hence, the large value of the objective function.

Effects of Economic Parameters

The variation of the objective function with respect to the state point temperature (T_1) for different thermoeconomic parameters (k_1 , k_2 and k_3) are shown in Figs.4(a-c). It is seen from these figures that the objective function first decreases and then increases as the state point temperature (T_1) increases. Thus, there is an optimal value of the state point temperature (T_1) at which the objective function attains its minimum for a given set of operating parameters and the optimum value of T_1 and hence the minima of the objective function will change if any operating parameter of the cycle is changed. Again the objective function goes up as any one of the economic parameters increases but the effects of k_2 and k_3 are more than those of k_1 on the objective function at the same set of operating condition.

Objective Function, Corresponding Power Output and Thermal Efficiency

Figures 5(a-c) show the $F \sim P_m^*$, $F \sim h_m$ and $P_m^* \sim h_m$ curves, which may be used to further reveal the performance characteristics of an irreversible Braysson cycle. It is seen from these figures that the objective function is not a monotonic function of the power output and thermal efficiency and hence, there are optimal values of the power output

and thermal efficiency at which the objective function attains its minimum values. Also the optimum operating regions of the objective function are situated in the regions of the $F \sim h_m$ and $F \sim P_m^*$ curves with positive slopes.

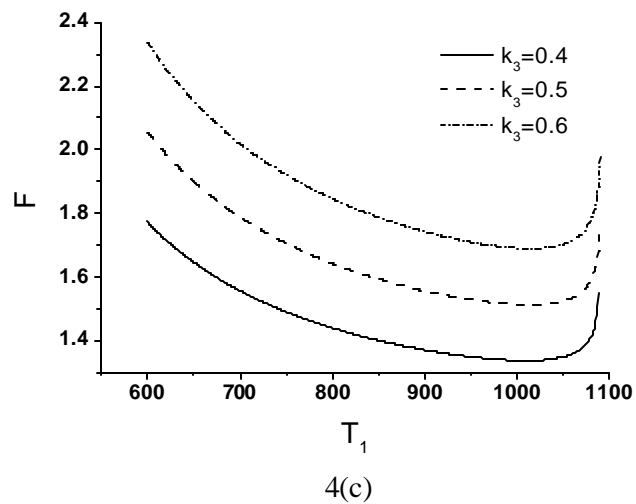
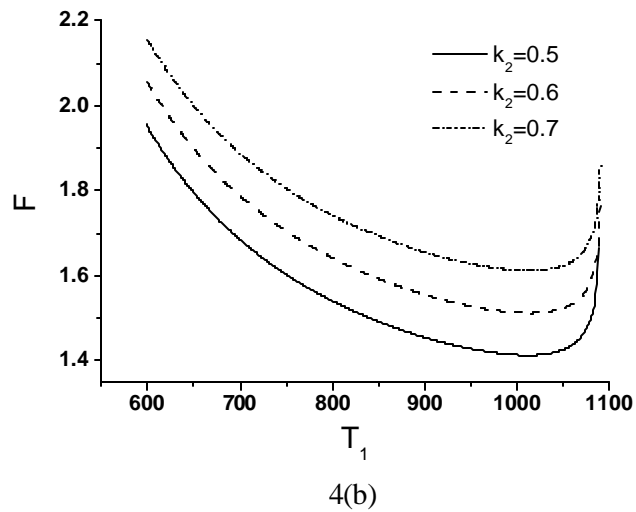
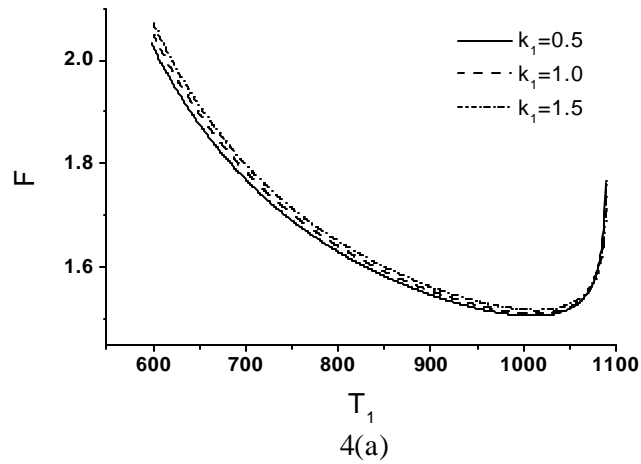
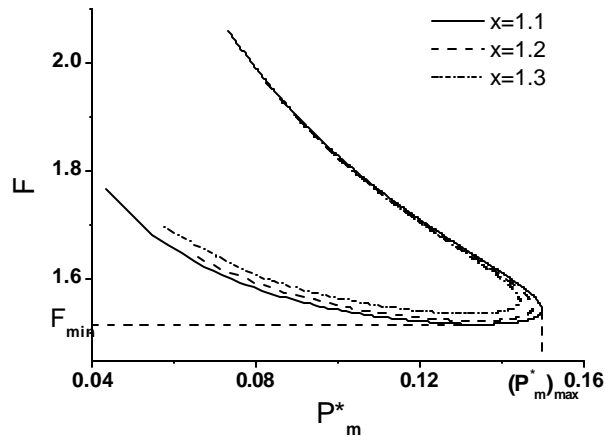
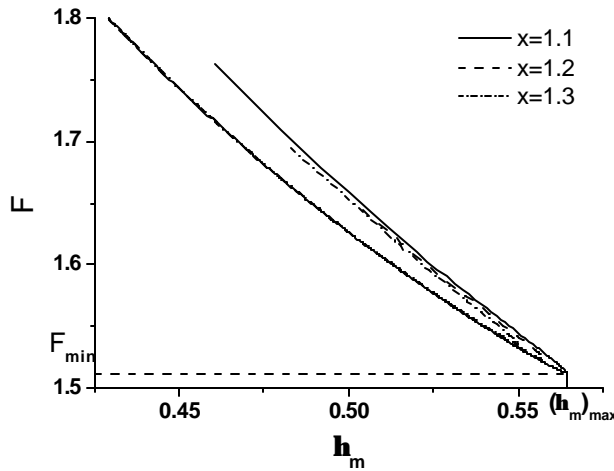


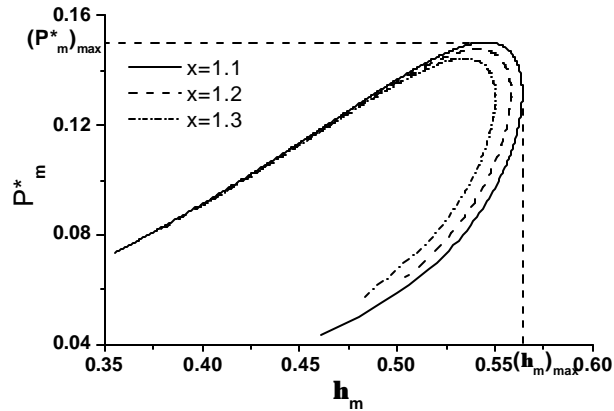
Fig.4. The variation of the objective function with respect to temperature T_1 for different parameters (a) k_1 , (b) k_2 and (c) k_3 , where $x=R=1.1$ and the values of the parameters are the same as those used in Fig. 2.



5(a)



5(b)



5(c)

Fig.5: The (a) $F \sim h_m$, (b) $F \sim P_m^*$ and (c) $P_m^* \sim h_m$ curves of a Braysson heat engine, where the values of the parameters are the same as those used in Fig. 2.

Again, it is seen from Fig.5(c) that the corresponding power output is not a monotonic function of the corresponding thermal efficiency. When the power output is situated in the regions of the $P_m^* \sim h_m$ curves with a positive slope, it will decrease as the thermal

efficiency is decreased. Obviously, these regions are not optimal. It is thus clear that the power output should be situated in the region of the $P_m^* \sim h_m$ curves with a negative slope. When the power output is in the region, it will increase as the thermal efficiency is decreased, and vice-versa. Thus, the optimal operating region of the objective function, power output and thermal efficiency are given by:

$$F_{\min} \leq (F_{opt})_{h_m} \leq (F_{opt})_{P_m^*} \tag{15}$$

$$(P_m^*)_{\max} \geq (P_m^*)_F \geq (P_m^*)_{h_m} \tag{16}$$

$$(h_m)_{\max} \geq (h_m)_F \geq (h_m)_{P_m^*} \tag{17}$$

This shows that $(P_m^*)_{\max}$, $(h_m)_{\max}$, $(P_m^*)_F$, $(h_m)_F$, $(P_m^*)_{h_m}$ and $(h_m)_{P_m^*}$ are the important optimal performance parameters of the Braysson heat engine. Thus $(P_m^*)_{\max}$ and $(h_m)_{\max}$ give the upper bounds of the power output and thermal efficiency at the minimized objective function, while $(P_m^*)_F$ and $(h_m)_F$ determine the values of the power output and thermal efficiency at the point of F_{\min} . On the other hand, $(P_m^*)_{h_m}$ and $(h_m)_{P_m^*}$ give the allowable values of the lower bounds of the power output and thermal efficiency at the minimized objective function.

According to Eqs.(8-9), we can further determine the optimal regions of other performance parameters. For example, the optimal regions of the parameters A_H / A and A_L / A may be, respectively, determined by:

$$(A_H / A)_{P_m^*} \leq (A_H / A)_F \leq (A_H / A)_{h_m} \tag{18}$$

$$(A_L / A)_{P_m^*} \geq (A_L / A)_F \geq (A_L / A)_{h_m} \tag{19}$$

where $(A_H / A)_F$, $(A_L / A)_F$, $(A_H / A)_{P_m^*}$, $(A_L / A)_{P_m^*}$ and $(A_H / A)_{h_m}$, $(A_L / A)_{h_m}$ are, respectively, the values of the A_H / A and A_L / A at the minimum objective function and the corresponding maximum specific power output and thermal efficiency.

So far we have obtained some optimum criteria for the important performance parameters of the cycle and found that the point of the minimum objective function is just in the optimal operating region, which may provide some important theoretical guidance for the design and improvement of an irreversible Braysson cycle.

A Special Case

When $x = 1$, the present cycle model becomes a finite time Carnot cycle [29-30] with internal irreversibility [31] and consequently, the performance of the Carnot cycle can be directly obtained from the above results as follows:

$$F_{\min} = \frac{1}{b_3 - Rb_4} \left[\frac{b_2 b_3 b_4}{b_4 - b_3 t} - Rk_2 b_4 + k_4 b_3 \right] \tag{20}$$

$$\frac{P_m}{(UA)_L} = \frac{b_1 (b_4 - b_3 t) (b_3 - Rb_4) T_H}{R(1+b_1) b_3 b_4} \tag{21}$$

$$h_m = (b_3 - Rb_4) \left(b_3 + \frac{u(1-t)(1+b_1)b_3 b_4}{b_4 - b_3 t} \left(1 + \frac{U_H R}{U_L b_1} \right) \right)^{-1} \tag{22}$$

$$T_{1,opt} = \frac{b_1 b_4 + b_3 t}{(1+b_1) b_4} T_H \tag{23}$$

$$T_{3,opt} = \frac{b_1 b_4 + b_3 t}{(1 + b_1) b_3} T_H \quad (24)$$

$$\frac{(UA)_H}{(UA)_L} = \frac{b_1}{R} \quad (25)$$

where $t = T_L / T_H$, $b_1 = \sqrt{Rk_6 / (1 + k_5)}$, $b_2 = (1 + k_5)(1 + b_1)^2 / T_H$, $b_3 = R(k_3 + b_2)$ and $b_4 = Rk_3 t + \sqrt{b_2 t (b_3 - R^2 k_3 t)}$

It is clear that the results obtained in Refs.[35, 36] may be directly derived from the above equations.

From these results mentioned above, we can conclude that the parameters viz. the objective function as well as the corresponding power output of the Carnot cycle is, respectively, smaller and larger than those of the Braysson cycle for the same set of operating parameters. Since, the objective function defined in this paper should be as less as possible (but not zero) from the point of view of economics for a given set of operating parameters. Thus, the Carnot cycle can exhibit better performance than the Braysson cycle for the same set of operating parameters not only from the point of view of thermodynamics but also from the point of view of thermoeconomics.

Conclusions

An irreversible cycle model of a Braysson heat engine is established and used to investigate the influence of multi-irreversibilities on the thermoeconomic objective function of the heat engine. The objective function is optimized with respect to the cycle temperatures for a given set of operating parameters. The minimum objective function and the corresponding power output as well as some other important parameters are calculated for a typical set of operating conditions. The optimal regions of some important parameters such as the objective function, corresponding power output and thermal efficiency, state point temperatures of the working fluid, heat-transfer area ratios, and so on, are determined in detail. The influence of the isobaric temperature ratio (x) and internal irreversibility parameter (R) on the performance of the cycle is analyzed. The objective function is found to be an increasing function of the internal irreversibility parameter, economic parameters and the isobaric temperature ratio. On the other hand, there exist the optimal values of the state point temperatures, power output and thermal efficiency at which the objective function attains its minimum for a typical set of operating parameters. A special case of the cycle is also discussed which indicates that the optimal thermoeconomic performance of an irreversible Carnot heat engine may be directly derived from the results obtained in this paper. In other words, the analysis presented in this paper is general and will be useful to understand the relationships and difference between the Braysson cycle and other cycles and to further improve the optimal design and operation from the point of view of economics as well as from the point of view of thermodynamics of a Braysson heat engine for the different set of operating parameters and for given constraints.

Acknowledgement: One of the authors (S K Tyagi) gratefully acknowledges the financial assistance and working opportunity provided by Xiamen University, Xiamen, People's Republic of China, during this study.

References

1. Frost, T. H.; Anderson, A.; Agnew, B. A hybrid gas turbine cycle (Brayton/Ericsson): an alternative to conventional combined gas and steam turbine power plant. *Proc. Inst. Mech. Eng. Part A* **1997**, 211, 121-131.
2. Zheng, T.; Chen, L.; Sun, F.; Wu, C. Power, power density and efficiency optimization of an endoreversible Brays son cycle. *Exergy* **2002**, 2, 380-386.
3. Zheng, J.; Chen, L.; Sun, F.; Wu, C. Powers and efficiency performance of an endoreversible Braysson cycle. *Int. J. Therm. Sci.* **2002**, 41, 201-205.
4. Wu, C.; Kiang, R. S. Work and power optimization of a finite time Brayton cycle. *Int. J. Ambient Energy* **1990**, 11, 129-136.
5. Wu, C.; Kiang, R. S. Power performance of a nonisentropic Brayton cycle, *J. Eng. Gas Turbines Power* **1991**, 113, 501-504.
6. Leff, H. S. Thermal efficiency at maximum power output: New results for old engines. *Am. J. Phys.* **1987**, 55, 602-610.
7. Ibrahim, O. M.; Klein, S. A.; Mitchell, J. W. Optimum heat power cycles for specified boundary conditions. *J. Eng. Gas Turbines Power* **1991**, 113, 514-521.
8. Wu, C. Specific power bounds of real heat engines. *Energy Convers. Mgmt.* **1991**, 31, 249-253.
9. Wu, C. Power optimization of an endoreversible Brayton gas heat engine. *Energy Convers. Mgmt.* **1991**, 31, 561-565.
10. Wu, C.; Chen, L.; Sun, F. Performance of a regenerative Brayton heat engine. *Energy* **1996**, 21, 71-76.
11. Cheng, C.Y.; Chen, C.K. Power optimization of an endoreversible regenerative Brayton cycle. *Energy* **1996**, 21, 241-247.
12. Chen, L.; Sun, F.; Wu, C.; Kiang, R. L. Theoretical analysis of the performance of a regenerative closed Brayton cycle with internal irreversibilities. *Energy Convers. Mgmt.* **1997**, 38, 871-877.
13. Radcenco, V.; Vargas, J. V. C.; Bejan, A. Thermodynamic optimization of a gas turbine power plant with pressure drop irreversibilities. *J. Energy Res. Tech.* **1998**, 129, 233-240.
14. Blank, D. A. Analysis of a combined law power optimized open Joule-Brayton heat engine cycle with a finite interactive heat source. *J. Phys. D: Appl. Phys.* **1999**, 32, 769-776.
15. Sahin, B.; Kodal, A.; Kaya, S. S. A comparative performance analysis of irreversible regenerative reheating Joule-Brayton heat engine under maximum power density and maximum power conditions. *J. Phys D: Appl. Phys.* **1998**, 31, 2125-2131.
16. Roco, J. M. M.; Velasco, S.; Medina, A.; Hernandez, A. C. Optimum performance of a regenerative Brayton thermal cycle. *J. Appl. Phys.* **1997**, 82, 2735-2741.
17. Feidt, M. Optimization of Brayton cycle engine in contract with fluid thermal capacities. *Rev. Gen. Them.* **1996**, 35, 662-666.
18. Chen, L.; Ni, N.; Cheng, G.; Sun F.; Wu, C. Performance of a real closed regenerated Brayton cycle via method of finite time thermodynamics. *Int. J. Ambient Energy*, **1999**, 20, 95-104.
19. Cheng, C. Y.; Chen, C. K. Power optimization of an irreversible Brayton heat engine. *Energy Sources* **1997**, 19, 461-474.
20. Blank, D. A.; Wu, C. A combined power optimized Joule-Brayton heat engine cycle with fixed thermal reservoir. *Int. J. Power and Energy* **2000**, 20, 1-6.
21. Frost, T. H.; Agnew, B.; Anderson, A. Optimizations for Brayton-Joule gas turbine cycles. *Proc. Inst. Mech. Eng. Part A: J. Power and Energy* **1992**, 206, 283-288.
22. Horlock, J. H.; Woods, W. A. Determination of the optimum performance of gas turbine. *Proc. Inst. Mech. Eng. Part C: J. Mech. Sci.* **2000**, 214, 243-255.

23. Kaushik, S. C.; Tyagi, S. K. Finite time thermodynamic analysis of an irreversible regenerative closed Brayton cycle heat engine. *Int. J. Solar Energy* **2002**, *22*, 141-151.
24. Blank, D. A.; Wu, C. Power limit of an endoreversible Ericsson cycle with regeneration. *Energy Convers. Mgmt.* **1996**, *37*, 59-66.
25. Blank, D. A.; Wu, C. Finite time power limit for solar-radiant Ericsson engines in space applications. *Appl. Therm. Eng.* **1998**, *18*, 1347-1357.
26. Chen, J.; Schouten, J. A. The comprehensive influence of several major irreversibilities on the performance of an Ericsson heat engine. *Appl. Therm. Eng.* **1999**, *19*, 555-564.
27. Tyagi, S. K. Application of finite time thermodynamics and second law evaluation of thermal energy conversion systems. Ph. D. Thesis, CCS. University, **2000**, Meerut, India.
28. Kaushik, S. C.; Kumar S. Finite time thermodynamic evaluation of irreversible Ericsson and Stirling heat engines. *Energy Convers. Mgmt.* **2001**, *42*, 295-312.
29. Curzon, F. L.; Ahlborn B. Efficiency of Carnot engine at maximum power output. *Am. J. Phys.* **1975**, *19*, 22-24.
30. Bejan, A. Theory of heat transfer irreversible power plants. *Int. J. Heat Mass Transfer* **1988**, *31*, 1211-1219.
31. Wu, C.; Kiang, R. L. Finite time thermodynamic analysis of a finite time Carnot heat engine with internal irreversibility. *Energy* **1992**, *17*, 1173-1178.
32. Chen, J. The maximum power output and maximum efficiency of an irreversible Carnot heat engine. *J. Phys. D: Appl. Phys.* **1994**, *27*, 1144-1149.
33. Chen, J. Thermodynamic and thermoeconomic analyses of an irreversible combined Carnot heat engine system. *Int. J. Energy Res.* **2001**, *25*, 413-426.
34. Kodal, A.; Sahin, B.; Yilmaz, T. Effects of internal irreversibility and heat leakage on the finite time thermoeconomic performance of refrigerators and heat pumps. *Energy Convers. Mgmt.* **2000**, *41*, 607-619.
35. Sahin, B.; Kodal, A. Performance analysis of an endoreversible heat engine based on a new thermoeconomic optimization criterion. *Energy Convers. Mgmt.* **2001**, *42*, 1085-1093.
36. Antar, M. A.; Zubair, S. M. Thermoeconomic considerations in the optimum allocation of heat exchanger inventory for a power plant. *Energy Convers. Mgmt.* **2001**, *42*, 1169-1179.